Heat transfer and fluid flow optimization of titanium dioxide–water nanofluids in a turbulent flow regime

Mehdi Mehrabi, Seyyed Mohammad Ali Noori Rahim Abadi, Josua Petrus Meyer

Department of Mechanical and Aeronautical Engineering, University of Pretoria, Pretoria, South Africa

Address correspondence to Dr. Mehdi Mehrabi, Department of Mechanical and Aeronautical Engineering, University of Pretoria, Private Bag X20, Hatfield, Pretoria, 0028, South Africa. E-mail: mehdi.mehrabi@up.ac.za Phone Number: 0 (+27) 12 420 4743, Fax Number: 0 (+27) 12 420 6632.

ABSTRACT

In this study, the convection heat transfer and pressure drop of titanium dioxide–water nanofluids were modeled by applying the fuzzy C-means adaptive neuro-fuzzy inference system (FCM-ANFIS) approach for a completely developed turbulent flow based on experimentally obtained training and test datasets. Two models were proposed based on the effective parameters; one model was developed for the Nusselt number considering the effects of the Reynolds number, Prandtl number, nanofluid volume concentration and average nanoparticle diameter. Another model was suggested for the pressure drop of the nanofluid as a function of the Reynolds number, nanofluid volume concentration, and average nanoparticle diameter. The results of these two proposed models were compared with experimental data as well as the existing correlations in the literature. The validity of the proposed models was benchmarked by statistical criteria. Moreover, a modified non-dominated sorting genetic algorithm (NSGA-II) multi-objective optimization technique was applied to obtain the optimum design points, and the final result was shown in a Pareto front.

INTRODUCTION

The paper published by Choi 1995 [1] was one of the first attempts to enhance the thermal conductivity performance of conventional fluids by adding nanoparticles to the base fluid. This new generation of heat transfer fluids was named nanofluids. Nanofluids are new heat transfer fluids that consist of two parts: a base fluid and nanometer-sized particles (1-100 nm). The latter can be metals, metal oxides, carbon nanotubes, a combination of different particles and newly suggested bio-nanoparticles. Nanofluids have received significant attention during the last decades and numerous researchers have worked on different aspects of nanofluids such as nanofluids synthesis [2–5], nanofluid thermophysical properties [6–9], heat transfer characteristics and pressure drop of nanofluids [10–13], and potential industrial application [14–16].

Because most of the industrial processes occur in a turbulent regime, studying of the heat transfer or pressure drop characteristics of nanofluids there is necessary to increase their use in practical applications.

Duangthongsuk and Wongwises [17] experimentally studied the heat transfer performance as well as friction factor of titanium dioxide–water nanofluids in a turbulent regime. They used nanoparticles with an average diameter of 21 nm to prepare nanofluids with a volume concentration ranging from 0.2 to 2%. It was shown that for the volume concentration of 1% the heat transfer coefficient increased by 26% compared with that of the base fluid. It was also observed that the pressure drop of this nanofluid was larger than of the base fluid at the same Reynolds number. In addition, the authors investigated the effect of the thermophysical property models of the nanofluids on the convection heat transfer and friction factor of low-concentration nanofluids [18]. They exhibited that using different models did not have a significant effect on the convection heat transfer performance of the titanium dioxide–water nanofluid with a volume concentration of 0.2%.

Sajadi and Kazemi [19] investigated the turbulent convective heat transfer characteristics and pressure drop of titanium dioxide–water nanofluids in a horizontal circular tube. Titanium dioxide nanoparticles with an average diameter of 30 nm were mixed with the base fluid (water) and sonicated for 30 min. After the nanofluid preparation, the Nusselt number and pressure drop of the nanofluids with volume concentrations below 0.25% were measured in a completely developed turbulent regime. It was demonstrated that the addition of small amounts of nanoparticles to water significantly enhanced the heat transfer of the titanium dioxide–water nanofluids. The pressure drop of the titanium dioxide–water nanofluids increased with the increase in the volume concentration, which was in the agreement with most of the results reported in the literature.

Abbasian Arani and Amani [20] performed an experimental investigation on the heat transfer and pressure drop of titanium dioxide nanoparticles with an average size of 30 nm dispersed in water serving as the base fluid. The experiments were performed in a turbulent flow regime for Reynolds number ranging from 8000 to 51000 and volume concentration ranging from 0.02 to 2%. They showed that for Reynolds numbers larger than 30000, more pumping power was required compared with that for low Reynolds numbers, whereas the Nusselt numbers were approximately equal.

Abbasian Arani and Amani [21] studied the effect of the nanoparticle diameter on the convective heat transfer characteristics and pressure drop of titanium dioxide–water nanofluids in a turbulent flow regime. To this end, nanoparticles with average diameters of 10, 20, 30, and 50 nm were dispersed in distilled acting as the base fluid and the Nusselt number and pressure drop of the titanium dioxide–water nanofluids were measured. The result of their experiments showed that the nanofluid with an average diameter of 20 nm had the best thermal performance compared with the other nanoparticles used in their experimental work.

The application of soft computing methods to model and analyze engineering problems has increased significantly during the last decade. Neural networks, fuzzy logic, and genetic algorithms are among the most preferred components of soft computing methods. These components are used in a wide range of mechanical engineering applications [22–25]. Because soft computing methods can recognize the existing knowledge and pattern behind empirical data, their application in modeling engineering problems of nanofluids has received remarkable attention during the last couple of years [26–29].

Aminossadati et al. [30] studied the laminar mixed convection of aluminum oxide–water nanofluids in a two-sided lid-driven cavity with a sliding top and bottom walls. In their research, a combination of adaptive neuro-fuzzy inference system (ANFIS) and computational fluid dynamics (CFD) techniques was used. Their results demonstrated that the ability of the ANFIS model to predict the fluid velocity, temperature and heat transfer of the cavity was similar to that of the CFD tool but with a much shorter computation time.

Balcilar et al. [31] utilized three different artificial neural networks to model the heat transfer coefficient and heat flux of the pool boiling of a titanium dioxide–water nanofluid. The ability of the artificial neural networks to predict the pool boiling heat transfer coefficient was tested by statistical criteria and experimental data. It was found that the radial basis function (RBF) neural network model results were in excellent agreement with the experimental data.

To obtain the best coolant for heat removal by different heat transfer equipment, Sayahi et al. [32] conducted an experimental study on the pool boiling heat transfer of three different nanofluids in the presence or absence of a surfactant. The pool boiling heat transfer of aluminum oxide–water, silicon dioxide–water, and zinc oxide–water nanofluids in a horizontal rod heater was measured experimentally. The experimental data were used to form

an RBF neural network model. The outcomes of the proposed RBF neural network model were in significant agreement with the experimental data.

The literature review revealed that no investigation has been conducted on the combination of the fuzzy C-means adaptive neuro-fuzzy inference system (FCM-ANFIS) modeling technique and modified non-dominated sorting genetic algorithm (NSGA-II) multi-objective optimization method for the modeling and optimization of the heat transfer and pressure drop of nanofluids. Therefore, the main objective of this study was to evaluate the applicability of this novel combination for predicting and optimizing the heat transfer and pressure drop of nanofluids. In this study, the Nusselt number and pressure drop of titanium dioxide–water nanofluids were modeled by using the FCM-ANFIS technique and four experimental datasets [17, 19–21]. The result was benchmarked with correlations available in the literature as well as statistical criteria. Moreover, the NSGA-II multi-objective optimization approach was used to obtain the Pareto front of the condensation heat transfer coefficient and pressure drop.

ADAPTIVE NEURO-FUZZY INFERENCE SYSTEM

ANFIS is a system that combines an artificial neural network and fuzzy logic methods to achieve a more robust modeling technique. In the ANFIS approach, the fuzzy logic transforms the qualitative knowledge to accurate quantitative analysis by a rule-based fuzzy inference system (FIS), whereas the neural network adjusts the membership functions and reduces the rate of errors of the rule determination process.

An ANFIS structure consists of introductory and concluding parts that are linked together by a set of rules. The multilayer structure of an ANFIS network has five distinct layers. The first layer of the ANFIS generates the fuzzy formation, and the second layer performs fuzzy “AND” and fuzzy rules. The third layer performs the normalization of the

membership functions. The fourth one is the conclusive part of the fuzzy rules, and finally, the last layer calculates the network outputs. A detailed information on the ANFIS structure layers is provided by Mehrabi et al. [33] and Rezazadeh et al. [34].

Three structure identification methods can be used for ANFIS: grid partitioning, subtractive clustering and fuzzy C-means (FCM) clustering [10]. In this study, the FCM clustering structure identification method was used to identify the premise membership functions for the ANFIS and final approach named FCM-ANFIS. The selection of the input variables, input space partitioning, choosing the membership functions, generation of the fuzzy rules, and selection of the initial parameters for the membership functions was conducted in the structure identification process [35].

Fuzzy C-Means Clustering algorithm

The FCM clustering algorithm was initially introduced by Dunn [36] and subsequently by Bezdek [37] and Bezdek et al. [38] as a data clustering technique in which each data point belongs to two or more clusters. The purpose of this unsupervised, iterative algorithm was to determine cluster centers based on the minimization of the sum of the weighted squares distance between each data point and the cluster centers.

In the FCM algorithm, first, the number of clusters v ($1 \leq v \leq n$) and fuzziness index (weighting exponent) m ($1 \leq m < \infty$) are selected randomly. Subsequent to the random selection of v and m, the algorithm starts by initializing the cluster centers, c_j , $j = 1, 2, \dots, v$, to a random value from n data points $\{x_1, x_2, \dots, x_n\}$. In the following step, the membership matrix $u_{ij} = [U]$, is computed by using Eq. (1)

$$u_{ij} = \frac{1}{\sum_{k=1}^{v} \left(\frac{\|x_i - c_j\|}{\|x_i - c_k\|} \right)^{\frac{2}{m-1}}} \quad (1)$$

$\|x_i - c_j\|, \|x_i - c_k\|$ are the Euclidean distances between the *j*-th and *k*-th cluster centers and *i*-th data point. After the computation of the membership matrix, objective function *J* is computed according to Eq. (2).

$$J(U, c_1, c_2, \ldots, c_v) = J_m = \sum_{i=1}^{n} \sum_{j=1}^{v} u_{ij}^m . \|x_i - c_j\|^2 \quad 1 \leq m < \infty \tag{2}$$

In the last step, new fuzzy cluster centers $c_j, j = 1, 2, \ldots, v$ are computed by using the following equation:

$$c_j = \frac{\sum_{i=1}^{n} u_{ij}^m . x_i}{\sum_{i=1}^{n} u_{ij}^m} \tag{3}$$

The basic algorithmic strategy of FCM is summarized below:

Fuzzy C-Means Clustering Algorithm
Step 1: randomly select the number of clusters and fuzziness index
Step 2: set termination criteria ε ($\varepsilon > 0$)
Step 3: initialize the cluster centers to a random value
Step 4: initialize the fuzzy membership function by using Eq.(1)
Step 5: compute the objective function (*J*) by using Eq.(2)
Step 6: compute the new cluster centers by using Eq.(3)
Step 7: repeat steps 4 to 6 until the objective function (*J*) is lower than the termination criteria

CONVECTIVE HEAT TRANSFER OF TITANIUM DIOXIDE–WATER NANOFLUIDS

The generation of unsteady vortexes during a turbulent flow regime coupled with a large contact area between the particles and fluid due to the addition of nanoparticles to the base fluid will significantly enhance the heat transfer. In view of this significant enhancement, investigations on the turbulent heat transfer of nanofluids are crucial for industrial applications. In this section, previous research on the convection heat transfer of titanium dioxide–water nanofluids in a turbulent flow regime is reviewed, and an FCM-ANFIS model for the Nusselt number is suggested.

In 1998, Pak and Cho [39] introduced the following correlation for the convection heat transfer of turbulent γ-aluminum oxide and titanium dioxide particles dispersed in water by curve-fitting of their experimental work:

$$Nu_{nf} = 0.021\, Re^{0.8} Pr^{0.5} \tag{4}$$

The Pak and Cho correlation was introduced under the experimental ranges of the volume concentration (0–3%), Reynolds number (10^4–10^5), and Prandtl number (6.54–12.33).

Duangthongsuk and Wongwises [17] introduced the following correlation for predicting the heat transfer coefficient of titanium dioxide–water nanofluids with volume concentrations ≤ 1.0% and Reynolds number ranging between 3000 and 18000:

$$Nu_{nf} = 0.074\, Re^{0.707} Pr^{0.385} \phi^{0.074} \tag{5}$$

Sajadi and Kazemi [19] proposed a correlation for the Nusselt number of titanium dioxide–water nanofluids in a completely developed turbulent regime as a function of the Reynolds and Prandtl numbers.

$$Nu_{nf} = 0.067\, Re^{0.71} Pr^{0.35} + 0.0005\, Re \tag{6}$$

The authors suggested that this correlation could be used for predicting the Nusselt number of titanium dioxide–water nanofluids with a volume concentration of 0.25% or lower and Reynolds numbers between 5000 and 30000.

Abbasian Arani and Amani [20] derived a correlation for the Nusselt number of titanium dioxide–water nanofluids with a nanoparticle volume fraction between 0.2% and 2%, and Reynolds number between 8000 and 51000 based on their experimental study on the effect of the nanoparticle volume fraction on the convection heat transfer characteristics of Titanium dioxide-water nanofluids as:

$$Nu_{nf} = 0.0041\, Re^{0.83} Pr^{1.35} (1 + \phi^{0.43}) \tag{7}$$

A year later, the above authors [21] introduced a new correlation by considering the effect of the average particle diameter of the nanoparticles on the convective heat transfer of

titanium dioxide–water nanofluids. Subsequent to the careful analysis of the experimental data obtained for four different average diameters of titanium dioxide nanoparticles, a correlation was proposed as a function of the Reynolds number, Prandtl number, nanoparticles volume concentration, and average particle size diameter.

$$Nu_{nf} = 0.006\, Re^{0.86} Pr\, \phi^{0.35} \left(\frac{D}{d_{bf}}\right)^{0.1} \quad , \begin{cases} d_{bf} = 0.386\ (nm) \\ \phi = 1\%, 1.5\%\ and\ 2\% \\ 8000 < Re < 55000 \end{cases} \tag{8}$$

where

$$D = -90 + 18.667\, d_p - 0.75\, d_p^2 + 0.00833\, d_p^3 \tag{9}$$

$$d_p = 10, 20, 30\ , and\ 50\ (nm)$$

Saha and Paul [40] after performing a numerical investigation on the heat transfer behavior of water-based alumina and titanium dioxide nanofluids in a turbulent flow regime, proposed a correlation for predicting the Nusselt number of Titanium dioxide-water nanofluids as a function of the Reynolds number ($1000 \leq Re \leq 10000$), Prandtl number ($8.42 \leq Pr \leq 20.29$) and nanoparticle size diameter (10 nm $\leq d_p \leq$ 40 nm). The correlation was as follows:

$$Nu_{nf} = 0.01259\, Re^{0.85926} Pr^{0.43020} \left(\frac{d_{bf}}{d_p}\right)^{-0.00068} \tag{10}$$

The above-mentioned correlation was used for the volume concentrations ranging from 4 to 6%.

Hejazian and Moraveji [41] numerically investigated the effect of the flow rate and nanofluid concentration on the Nusselt number of titanium dioxide–water nanofluids. By using the mixture model results, they developed the following correlation between the Reynolds number ($4800 \leq Re \leq 30500$), Prandtl number ($5.5 \leq Pr \leq 5.59$), and volume concentration ($0 \leq \phi \leq 0.25\%$):

$$Nu_{nf} = 0.00218\, Re^{1.0037} Pr^{0.5} \left[1 + \left(\frac{\phi}{100}\right)\right]^{154.6471} \quad (11)$$

Table 1 summarizes the proposed correlations for the prediction of the Nusselt number of the titanium dioxide–water nanofluids.

In this section, some of the significant studies on the convection heat transfer of titanium dioxide–water nanofluids in turbulent flow regimes reported in the literature are reviewed. After a careful review of these papers, it was realized that only a few of researchers considered the average diameters of the nanofluids as effective parameters for the Nusselt number. In comparison, almost all of them considered the effect of the Reynolds number and volume concentration. By using the experimental results of Duangthongsuk and Wongwises [17], Sajadi and Kazemi [19] and Abbasian Arani and Amani [20 and 21] and the FCM-ANFIS technique, a model was developed to predict the Nusselt number of titanium dioxide–water nanofluids in a turbulent flow regime as a function of the Reynolds number, Prandtl number, volume concentration and average particle size. The results of the proposed model were compared with the experimental data [17, 19–21] and above-mentioned correlations.

PRESSURE DROP OF TITANIUM DIOXIDE–WATER NANOFLUIDS

In the literature, it is widely accepted that adding nanoparticles to a base fluid will increase its viscosity and affect the pressure drop. Therefore, the study of the pressure drop of these nanofluids is essential for the acceleration of their usage in industrial applications.

An FCM-ANFIS model based on the experimental results of Duangthongsuk and Wongwises [17], Sajadi and Kazemi [19] and Abbasian Arani and Amani [20 and 21] was developed to predict the pressure drop of titanium dioxide–water nanofluids in a turbulent flow regime as a function of the Reynolds number, nanoparticle volume concentration and average particle size.

MULTI-OBJECTIVE OPTIMIZATION

The majority of engineering applications deal with different objectives that generally compete with each other. The best example of this is in the heat transfer engineering problems, where normally the attempts to increase the heat transfer result in a larger pressure drop, which is not desirable. Multi-objective optimization techniques are the answer to those engineering problems that involve more than one objective function or conflicting objective functions.

Multi-objective optimization problems involve more than one and often competing objective functions to be optimized simultaneously. For the majority of the applications in heat and fluid sciences, the search is for higher heat transfer while simultaneously avoiding an increase in the pressure drop or apparatus size. For these types of problems, where maximizing one favorable objective function will result in an unfavorable increase in the other objective functions, the only approach is to use multi-objective optimization techniques. In a multi-objective optimization, a single optimized solution does not exist; instead, the result is in the form of a set of optimized solutions called the Pareto front or Pareto optimal points, where the values of none of the objective functions can be improved without degrading one or more of the other objective values.

Various multi-objective algorithms have been applied to engineering in the last two decades. Among them, the NSGA-II algorithm, which was first introduced by Deb et al. [42], is one of the most effective approaches and has been chosen for this research.

The NSGA-II algorithm has different operators that should work together to generate a robust multi-objective optimization technique. The information in the operators including the fast non-dominated sorting operator, crowding-distance-assignment operator, and simulated binary crossover (SBX) operator, their connections to each other, and flow diagram of the algorithm are given in [42–43]. In this study, the condensation heat transfer coefficient and

pressure drop are two competing objectives. The objective of the optimization process in this study is to obtain the best design variables to simultaneously maximize the Nusselt number and minimize the pressure drop with respect to the Reynolds number, Prandtl number, volume concentration and average particle size, which are the design variables.

RESULTS AND DISCUSSION

A total number of 162 input–output experimental data points obtained from the literature [17, 19–21] were used to predict the Nusselt number for titanium dioxide–water nanofluids. The experimental data were divided into two subsets as 129 data points for training and 33 data points for testing purposes. To model the pressure drop, 153 experimental data points from [17, 19–21] were divided into two subsets as 125 data points for training and 28 data points for testing purposes.

The optimum ANFIS structure and membership functions were obtained by the FCM clustering technique, in which the input variables were fuzzied with Gaussian membership functions labeled MF1–MF15 for the Nusselt number of the titanium dioxide–water nanofluids and MF1–MF10 for the pressure drop of the titanium dioxide–water nanofluids. The parameters of these membership functions are listed in Tables 3 and 4 for the Nusselt number and pressure drop of the titanium dioxide–water nanofluids, respectively.

The fuzzy rule base and outputs of our proposed FCM-ANFIS models are listed in Tables 5 and 6, respectively. The resultant optimum parameters obtained after the ANFIS training process are provided in the Appendix.

The mean absolute error (*MAE*), mean relative error (*MRE*) and root mean square errors (*RMSE*) criteria were used as listed in Table 1, to exhibit the accuracy of our proposed FCM-ANFIS models to predict the Nusselt number and pressure drop of the titanium dioxide–water nanofluids.

Figure 1 shows the experimental results of Sajadi and Kazemi [19] for a titanium dioxide–water nanofluid with an average nanoparticle size of 30 nm and volume concentration of 0.1% compared with the proposed FCM-ANFIS model for the Nusselt number of the titanium dioxide–water nanofluid. Four correlations defined by Pak and Cho [39], Duangthongsuk and Wongwises [17], Abbasian Arani and Amani [20], and Hejazian and Moraveji [41] are also compared with the experimental data and proposed FCM-ANFIS model. The FCM-ANFIS result for the Nusselt number exhibit a very good agreement with the experimental data (*MAE* = 1.1, *MRE* = 1.4%, and *RMSE* = 1.2). The model matches with the experimental data very well and predicts the Nusselt number better than all the mentioned correlations.

The experimental results of Duangthongsuk and Wongwises [17] for the Nusselt number of a titanium dioxide–water nanofluid with an average nanoparticle size of 21 nm and volume concentration of 0.6% are shown in Figure 2. The FCM-ANFIS model output and three applicable correlations for the particle size of 21 nm and volume concentration of 0.6% for the Reynolds numbers ranging from 4500 to 14500 are also presented. The results reveal that the FCM-ANFIS model is in good agreement with the experimental data (*MAE* = 3.6, *MRE* = 4.1%, and *RMSE* = 4.1). The correlations defined by Sajadi and Kazemi [19] and Abbasian Arani and Amani [20] predict the Nusselt number to be very good for Reynolds numbers larger than 8000. The Pak and Cho [39] correlation cover the Reynolds numbers less than 10000 but cannot predict the experimental results well.

In Figures 3 and 4, the experimental results of Abbasian Arani and Amani [21] are compared with those of the FCM-ANFIS model and correlations for the Nusselt number of titanium dioxide–water nanofluids with particle sizes of 50 nm and 10 nm and volume concentrations of 1.5% and 2%, respectively. In Figure 3, the FCM-ANFIS exhibits a very good prediction ability and the model is well matched with the experimental data (*MAE* =

6.8, *MRE* = 3.9%, and *RMSE* = 8.2) and (*MAE* = 9, *MRE* = 4.7%, and *RMSE* = 9.5), Figure 4 also shows that the FCM-ANFIS model is in good agreement with the experimental data (*MAE* = 9, *MRE* = 4.7%, and *RMSE* = 9.5) and predicts the Nusselt number the best, whereas the Abbasian Arani and Amani [20] correlation significantly under-predicts the experimental data.

Figures 1–4 illustrate that the FCM-ANFIS predicts the Nusselt number of the titanium dioxide–water nanofluids significantly better than the correlations in the literature, and in all the cases, the proposed model outcome and experimental data match.

Figure 5a exhibits the comparison between the experimental results of Sajadi and Kazemi [19] and FCM-ANFIS model for the pressure drop of a titanium dioxide–water nanofluid with a particle size of 30 nm and volume concentration of 0.15%. The FCM-ANFIS model predicts the experimental results very well (*MAE* = 0.32, *MRE* = 4.7%, and *RMSE* = 0.34).

In Figure 5b, the experimental results of Duangthongsuk and Wongwises [17] are compared with those of the FCM-ANFIS model for the pressure drop of a titanium dioxide–water nanofluid with a particle size of 21 nm and volume concentration of 0.2%. The FCM-ANFIS model does not predict the pressure drop the best among the considered measurements (*MAE* = 0.59, *MRE* = 13.7%, and *RMSE* = 0.53). The proposed model predicts the pressure drop of the nanofluid better for Reynolds numbers less than 8000, whereas for Reynolds number larger than 11000, it considerably under-predicts the experimental results.

Figure 5c presents shows the comparison of the experimental results of Abbasian Arani and Amani [21] and FCM-ANFIS model for a particle size of 50 nm and volume concentration of 1%. The FCM-ANFIS model is not in a good agreement with the experimental data for Reynolds numbers less than 35000 but it predicts very well for large Reynolds numbers. The overall prediction ability of the model is acceptable (*MAE* = 1.2, *MRE* = 11.8%, and *RMSE* = 1.5).

In Figure 5d, the experimental result of Abbasian Arani and Amani [21] is compared with that of the FCM-ANFIS model for a particle size of 10 nm and volume concentration of 1.5%. The FCM-ANFIS model matches the experimental data well (*MAE* = 0.92, *MRE* = 12.6%, and *RMSE* = 1.14).

Optimum operating conditions

Figure 6 presents the Pareto front of the Nusselt number and pressure drop of the titanium oxide–water nanofluids. All the presented points (Pareto sets) in this figure are the optimum points corresponding to different operating conditions. The results are divided into two different regions, I and II. The corresponding design variables (input variables) as well as objective functions for the four points (A, B, C, and D) corresponding to the start and end points of regions I and II are listed in Table 7.

The values of the Nusselt numbers are small region I, varying from 207.856 for point A to 265.599 for point B, with a pressure drop between 1.187 and 4.629 kPa. Therefore, the ultimate optimum operating conditions are not located in region I. In Section I, which starts at point A and ends at B, the Nusselt number increases by 28% (from 207.856 to 265.599) when the pressure drop increases by 290% (from 1.187 kPa to 4.629 kPa). In the search for a small pressure drop, points closer to point A are the best options but owing to the small Nusselt number points in this region cannot be optimum.

Region II starts (Point C) with practically the same values of the Nusselt number and pressure drop of the end point of section I (Point B). However, at the end of this region, the value of the Nusselt number shows an 89% increase from 274.492 to 519.964, whereas for the same region, the pressure drop increases by 74% from 5.197 kPa to 9.027 kPa.

The results show that selecting the final design points from region II is a better option than region I. However, it is important to note that all the points in this Pareto front are optimal

points. The final optimum point depends on the designer requirement and may vary based on the weight of each objective function.

CONCLUSION

In the present study, the FCM-ANFIS technique was used for the modeling and optimization of the convective heat transfer coefficient and pressure drop of titanium dioxide–water nanofluids in a turbulent flow regime. An input–output experimental dataset was used to model the Nusselt number and pressure drop as a function of the effective parameters: Reynolds number, Prandtl number, nanoparticle volume concentration, and average nanoparticle diameter. From this research, the following conclusions can be drawn:

I. The result predicted by the proposed FCM-ANFIS models showed an excellent agreement with the experimental data. The maximum mean relative error (MRE) of the predicted results for the Nusselt number and pressure drop was 4.7% and 13.7%, respectively.

II. Although the general trends of the empirical correlations were similar to those of the proposed model for the Nusselt number, they often exhibited significant deviations relative to the experimental data. This can be attributed to the fact that the proposed empirical correlations were based on specific experimental results and so, could not be generalized to all the cases.

III. The multi-objective optimization results, presented two distinct regions. Even though the selection of the optimum point depended on the designer requirements, selecting choosing the final design points from region II was a better option than from region I.

APPENDIX

$$[\mathbf{a}_{i,j}] = \begin{bmatrix} 6.444 & 1.06 & 0.006189 & 6.921 & -40.08 \\ -184.2 & 20.69 & -0.01053 & -206.6 & 187.7 \\ 34.06 & -2.777 & 0.01674 & -5.601 & 16.02 \\ -212.8 & 6.575 & 0.007908 & -84.95 & 440 \\ 708.7 & 2.87 & -0.04242 & 154.7 & 34.87 \\ 123.8 & 3.223 & 0.003876 & 151.9 & -553.9 \\ 428.2 & -0.3784 & 0.01136 & 194.6 & -1155 \\ 92.79 & -1.036 & 0.007783 & 83.96 & -405 \\ 74.3 & -0.9992 & 0.007398 & 119.7 & -478.8 \\ 32.85 & 0.2868 & -0.01205 & 24.65 & -216.9 \\ -413.8 & -66.05 & -0.00277 & 557.7 & -282.3 \\ 97.96 & -6.333 & 0.002565 & 70.8 & -14.67 \\ 22.1 & 12.87 & -0.01146 & 513.5 & -1645 \\ -72.37 & 1.143 & -0.00245 & -167.9 & 931.1 \\ 27.61 & -2.269 & 0.004854 & 35.57 & -1.974 \end{bmatrix}$$

$$[\mathbf{b}_{i,j}] = \begin{bmatrix} 5.059 & -0.06457 & 0.000876 & -22.23 \\ 26.22 & -0.0077 & 0.000936 & -45.24 \\ 3.277 & -0.1322 & 0.001228 & -30.15 \\ 4.485 & -0.01561 & 0.001166 & 2.832 \\ 5.059 & 12.44 & -0.00395 & -209.5 \\ 9.898 & -0.3202 & 0.002164 & -52 \\ -5.198 & -15.69 & 0.005577 & 388.7 \\ -9.089 & 0.1311 & 0.000427 & 4.353 \\ 4.424 & -0.1554 & 0.001702 & -39.02 \\ 2.656 & -0.1059 & 0.000623 & -6.428 \end{bmatrix}$$

NOMENCLATURE

a_i	polynomial coefficient (weight)
ANFIS	fuzzy C-means adaptive neuro-fuzzy inference system
dp	nanoparticle average diameter, nm
D	modified nanoparticle average diameter, nm
Nu	Nusselt number
ΔP	pressure drop, kPa
Pr	Prandtl number
Re	Reynolds number
c	cluster centres
J	objective function
U	fuzzy membership matrix
uij	fuzzy membership function
v	number of clusters
x	data point
m	fuzziness index
M	Gaussian fuzzy membership function center
MAE	mean absolute error
MRE	mean relative error
n	Gaussian fuzzy membership function width
NSGA	Non-dominated sorting genetic algorithm
RMSE	root mean squared error
Xp	predicted value
Xa	actual (experimental) data

Greek symbols

ϕ volume concentration, %

Subscripts

nf nanofluid

bf base fluid

REFERENCES

[1] Choi, S.U.S., Enhancing Thermal Conductivity of Fluids with Nanoparticles, *ASME FED*, vol. 231, pp. 99–103, 1995.

[2] Moon, Y.K. , Lee, J., Lee, J.K., Kim, T.K., Kim S.H., Synthesis of Length-Controlled Aerosol Carbon Nanotubes and Their Dispersion Stability in Squeous Solution, *Langmuir*, vol. 25, no. 3, pp. 1739-1743, 2009.

[3] Agarwal, D.K., Vaidyanathan, A., Kumar, S.S., Synthesis and Characterization of Kerosene-Alumina Nanofluids, *Applied Thermal Engineering*, vol.60, no. (1-2), pp. 275-284 , 2013.

[4] Heo, Y.K., Bratescu, M.A., Ueno, T., Saito, T.N., Synthesis of Mono-Dispersed Nanofluids Using Solution Plasma, *Journal of Applied Physics*, vol. 116, no. 2, pp. 024302, 2014.

[5] Kamatchi, R., Venkatachalapathy, S., Abhinaya Srinivas, B., Synthesis, Stability, Transport Properties, and Surface Wettability of Reduced Graphene Oxide/Water Nanofluids, *International Journal of Thermal Science*, vol. 97, pp. 17-25, 2015.

[6] Avsec, J., Oblak, M., The Calculation of Thermal Conductivity, Viscosity and Thermodynamic Properties for Nanofluids on the Basis of Statistical Nanomechanics, *International Journal of Heat and Mass Transfer*, vol.50, no.(21-22), pp. 4331-4341, 2007.

[7] Gu, B., Wang, Z., Lu, Z., Chen, S., Investigation of Thermal Conductivity of Nanofluids Using Different Experimental Methodologies, *Advanced Materials Research*, vol.468-471, pp. 2042-2046 , 2012.

[8] Huminic, G., Huminic, A., Dumitrache, F., Fleaca, C., Morjan, I.,Experimental Study of Thermo-Physical Properties of Nanofluids Based on γ-Fe_2O_3 Nanoparticles for Heat Transfer Applications, *Heat Transfer Engineering*, vol. 38, no. 17, pp. 1469-1505, 2017.

[9] Mechiri, S.K., Vasu, V., Venu Gopal, A., Investigation of Thermal Conductivity and Rheological Properties of Vegetable Oil Based Hybrid Nanofluids Containing Cu–Zn Hybrid Nanoparticles, *Experimental Heat Transfer*, vol.30, no. 3, pp. 205-217, 2017.

[10] Rea, U., McKrell, T., Hu, L.W., Buongiorno, J., Laminar Convective Heat Transfer and Viscous Pressure Loss of Alumina-Water and Zirconia-Water Nanofluids, *International Journal of Heat and Mass Transfer*, vol.52, no. (7-8), pp. 2042-2048, 2009.

[11] Saxena, R., Gangacharyulu, D., Bulasara, V.K., Heat Transfer and Pressure Drop Characteristics of Dilute Alumina–Water Nanofluids in a Pipe at Different Power Inputs, *Heat Transfer Engineering*, vol. 37, no. 18, pp. 1554-1565, 2016.

[12] Chougule, S.S., Nirgude, V.V., Sahu, S.K., Experimental Study on Laminar Forced Convection of Al_2O_3/Water and Multiwall Carbon Nanotubes/Water Nanofluid of Varied Particle Concentration with Helical Twisted Tape Inserts in Pipe Flow, *Heat Transfer Engineering*, vol, 0, no. 0, pp. 1-13, 2017.

[13] Goharkhah, M., Ashjaee, M., Shahabadi, M., Experimental Investigation on Convective Heat Transfer and Hydrodynamic Characteristics of Magnetite Nanofluid Under the Influence of an Alternating Magnetic Field, *International Journal of Thermal Sciences*, vol. 99, pp. 113-124, 2016.

[14] Yahya, N., Kashif, M., Nasir, N., Akhtar, M.N., Yusof, N.M., Cobalt Ferrite Nanoparticles: An Innovative Approach for Enhanced Oil Recovery Application, *Journal of Nano Research*, vol. 17, pp. 115-126, 2012.

[15] Peyghambarzadeh, S.M., Hashemabadi, S.H., Naraki, M., Vermahmoudi, Y., Experimental Study of Overall Heat Transfer Coefficient in the Application of Dilute Nanofluids in the Car Radiator, *Applied Thermal Engineering*, vol. 52, no. 1, pp. 8-16, 2013.

[16] Tripathi, D., Bég, O.A., A study on Oeristaltic Flow of Nanofluids: Application in Drug Delivery Systems, *International Journal of Heat and Mass Transfer*, vol. 70, pp. 61-70, 2014.

[17] Duangthongsuk, W., Wongwises, S., An Experimental Study on the Heat Transfer Performance and Pressure Drop of TiO_2-water Nanofluids Flowing Under a Turbulent Flow Regime, *International Journal of Heat and Mass Transfer*, vol. 53, pp. 334-344, 2010.

[18] Duangthongsuk, W., Wongwises, S., Effect of Thermophysical Properties Models on the Prediction of the Convective Heat Transfer Coefficient for Low Concentration Nanofluid, *International Communications in Heat and Mass Transfer*, vol. 35, no. 10, pp. 1320-1326, 2008.

[19] Sajadi, A.R., Kazemi, M.H., Investigation of Turbulent Convective Heat Transfer and Pressure Drop of TiO_2/water Nanofluid in Circular Tube, *International Communications in Heat and Mass Transfer*, vol. 38, pp. 1474-1478, 2011.

[20] Abbasian Arani, Amani, J., Experimental Study on the Effect of TiO_2–water Nanofluid on Heat Transfer and Pressure Drop, *Experimental Thermal and Fluid Science*, vol. 42, pp. 107-115, 2012.

[21] Abbasian Arani, Amani, J., Experimental Investigation of Diameter Effect on Heat Transfer Performance and Pressure Drop of TiO_2–water Nanofluid, *Experimental Thermal and Fluid Science*, vol. 44, pp. 520-533, 2013.

[22] Tam, L.M., Ghajar, A.J., Tam, H.K., Contribution Analysis of Dimensionless Variables for Laminar and Turbulent Flow Convection Heat Transfer in a Horizontal Tube Using Artificial Neural Network, *Heat Transfer Engineering*, vol. 29, no. 9, pp. 793-804, 2008.

[23] Gosselin, L., Tye-Gingras, M., Mathieu-Potvin, F., Review of Utilization of Genetic Algorithms in Heat Transfer Problems, *International Journal of Heat and Mass Transfer*, vol. 52, no. (9-10), pp. 2169-2188, 2009.

[24] Khan, W.A., Kadri, M.B., Qasim, A.,Optimization of Microchannel Heat Sinks Using Genetic Algorithm, *Heat Transfer Engineering*, vol. 34, no. 4, pp. 279-287, 2013.

[25] Mazalan, N.A., Malek, A.M., Wahid, M.A., Mailah, M., Sensitivity Analysis on Neural Network Algorithm for Primary Superheater Spray Modeling, *Heat Transfer Engineering*, vol. 38, no. 4, pp. 417-422, 2017.

[26] Santra, A.K., Chakraborty, N., Sen, S., Prediction of Heat Transfer Due to Presence of Copper–water Nanofluid Using Resilient-propagation Neural Network, *International Journal of Thermal Sciences*, vol. 48, pp. 1311-1318, 2009.

[27] Shanbedi, M., Amiri, A., Rashidi, S., Zeinali Heris S.,Baniadam M., Thermal Performance Prediction of Two-Phase Closed Thermosyphon Using Adaptive Neuro-Fuzzy Inference System, *Heat Transfer Engineering*, vol. 36, no. 3, pp. 315-324, 2015.

[28] Adio, S.A., Mehrabi, M., Sharifpur, M., Meyer, J.P., Experimental Investigation and Model Development for Effective Viscosity of MgO-Ethylene Glycol Nanofluids by Using Dimensional Analysis, FCM-ANFIS and GA-PNN Techniques, *International Communications in Heat and Mass Transfer*, vol. 72, pp. 71-83, 2016.

[29] Sadi, M., Prediction of Thermal Conductivity and Viscosity of Ionic Liquid-Based Nanofluids Using Adaptive Neuro Fuzzy Inference System, *Heat Transfer Engineering*, vol. 38, no. 18, pp. 1561-1572, 2017.

[30] Aminossadati, S.M., Kargar, A., Ghasemi, B., Adaptive Network-Based Fuzzy Inference System Analysis of Mixed Convection in a Two-Sided Lid-Driven Cavity Filled with a Nanofluid, *International Journal of Thermal Sciences*, vol. 52, pp. 102-111, 2012.

[31] Balcilar, M., Dalkilic, A., Suriyawong, A., Yiamsawas, T., Wongwises, S., Investigation of Pool Boiling of Nanofluids Using Artificial Neural Networks and Correlation Development Techniques, *International Communications in Heat and Mass Transfer,* vol. 39, pp. 424-431, 2012.

[32] Sayahi, T., Tatar, A., Bahrami, M., A RBF Model for Predicting the Pool Boiling Behavior of Nanofluids Over a Horizontal Rod Heater, *International Journal of Thermal Sciences,* vol. 99, pp. 180-194, 2016.

[33] Mehrabi, M., Pesteei, S.M., Pashaee, T., Modeling of Heat Transfer and Fluid Flow Characteristics of Helicoidal Double-Pipe Heat Exchangers Using Adaptive Neuro-Fuzzy Inference System (ANFIS), *International Communications in Heat and Mass Transfer*, vol. 38, no. 4, pp. 525-532, 2011.

[34] Rezazadeh, S., Mehrabi, M., Pesteei, S.M., Mirzaee, I., Using Adaptive Neuro-Fuzzy Inference System (ANFIS) for Proton Exchange Membrane Fuel Cell (PEMFC) Performance Modeling, *Journal of Mechanical Science and Technology*, vol. 26, no. 11, pp. 3701-3709, 2012.

[35] Jalalifar, H., Mojedifar, S., Sahebi, A.A., Nezamabadi-pour, H., Application of the Adaptive Neuro-Fuzzy Inference System for Prediction of a Rock Engineering Classification System, *Computers and Geotechnics*, vol. 38, pp. 783-790, 2011.

[36] Dunn, J.C., A Fuzzy Relative of the ISODATA Process and Its Use in Detecting Compact Well-Separated Clusters, *Journal of Cybernetics*, vol. 3, no. 3, pp. 32-57, 1973.

[37] Bezdek, J. C., *Pattern Recognition with Fuzzy Objective Function Algorithms*, pp. 256, Plenum, New York, 1981.

[38] Bezdek, J.C., Ehrlich, R., Full, W., FCM: The Fuzzy C-Means Clustering Algorithm. *Computers & Geosciences*, vol. 10, no. (2-3), pp. 191-203, 1984.

[39] Pak, B.C., Cho, Y.I., Hydrodynamic and Heat Transfer Study of Dispersed Fluids with Submicron Metallic Oxide Particles, *Experimental Heat Transfer*, vol. 11, no. 2, pp. 151-170, 1998.

[40] Saha, G., Paul, M.C., Numerical Analysis of the Heat Transfer Behaviour of Water Based Al_2O_3 and TiO_2 Nanofluids in a Circular Pipe Under the Turbulent Flow Condition, *International Communications in Heat and Mass Transfer*, vol. 56, pp. 96-108, 2014.

[41] Hejazian, M., Keshavarz Moraveji, M., A Comparative Analysis of Single and Two-Phase Models of Turbulent Convective Heat Transfer in a Tube for TiO_2 nanofluid with CFD, *Numerical Heat Transfer, Part A*, vol. 63, pp. 795–806, 2013.

[42] Deb, K., Pratap, A., Agarwal, S., Meyarivan, T., A Fast and Elitist Multiobjective Genetic Algorithm: NSGA-II, *IEEE Transactions on Evolutionary Computation*, vol. 6, pp. 182-197, 2002.

[43] Hamdan, M., A Dynamic Polynomial Mutation for Evolutionary Multi-objective Optimization Algorithms, *International Journal on Artificial Intelligence Tools*, vol.20, no.1, pp. 209-219, 2011.

Table 1 Convective heat transfer correlations for Titanium dioxide-water nanofluids

Reference	Equation	Conditions
Pak and Cho [39]	$Nu_{nf} = 0.021\, Re^{0.8} Pr^{0.5}$	1000 < Re < 10000 6.54 < *Pr* < 12.33 0 < ϕ ≤ 3%
Duangthongsuk and Wongwises [17]	$Nu_{nf} = 0.074\, Re^{0.707} Pr^{0.385} \phi^{0.074}$	3000 < Re < 18000 1.5 < *Pr* < 7.5 ϕ ≤ 1%
Sajadi and Kazemi [19]	$Nu_{nf} = 0.067\, Re^{0.71} Pr^{0.35} + 0.0005\, Re$	5000 < Re < 30000 1.7 < *Pr* < 2.5 0 < ϕ ≤ 0.25%
Abbasian Arani and Amani [20]	$Nu_{nf} = 0.0041\, Re^{0.83} Pr^{1.35} (1 + \phi^{0.43})$	8000 < Re < 51000 3.2 < *Pr* < 4.5 0.2% ≤ ϕ ≤ 2%
Abbasian Arani and Amani [21]	$Nu_{nf} = 0.006\, Re^{0.86} Pr\, \phi^{0.35} (\frac{D}{d_{bf}})^{0.1}$ Where D = -90+18.667 d_p -0.75 d_p^2+ 0.00833 d_p^3	8000 < Re < 55000 3.2 < *Pr* < 4.5 ϕ = 1%, 1.5% and 2% d_{bf} = 0.386 nm d_p=10, 20, 30 and 50 nm
Saha and Paul [40]	$Nu_{nf} = 0.01259\, Re^{0.85926} Pr^{0.43020} (\frac{d_{bf}}{d_p})^{-0.00068}$	1000 ≤ *Re* ≤ 10000 4% ≤ ϕ ≤ 6% 10 nm ≤ d_p ≤ 40 nm 8.42 ≤ *Pr* ≤ 20.29
Hejazian and Moraveji [41]	$Nu_{nf} = 0.00218\, Re^{1.0037} Pr^{0.5} \left[1 + \left(\frac{\phi}{100}\right)\right]^{154.6471}$	4800 ≤ *Re* ≤ 30500 0 ≤ ϕ ≤ 0.25% 5.5 ≤ *Pr* ≤ 5.59

Table 2 Statistical criteria used for the analysis of the results

Statistical criterion	Equation
Mean absolute error	$MAE = \frac{1}{n}\sum_{i=1}^{n}\left\|X_p - X_a\right\|$
Mean relative error	$MRE(\%) = \frac{100}{n}\sum_{i=1}^{n}\left(\frac{\left\|X_p - X_a\right\|}{X_a}\right)$
Root mean square error	$RMSE = \sqrt{\frac{1}{n}\sum_{i=1}^{n}\left(X_p - X_a\right)^2}$

Table 3 Parameters of the membership functions for modeling the Nusselt number of the titanium dioxide–water nanofluids

Membership function	Input 1 ϕ (%)		Input 2 d_p(nm)		Input 3 *Re*		Input 4 *Pr*	
	n	*M*	*n*	*M*	*n*	*M*	*n*	*M*
MF1	1.123	0.79	10.9	23.67	4395	5274	2.939	3.927
MF2	0.4352	0.9124	5.675	32	3174	20170	0.3583	2.808
MF3	0.5198	1.473	9.194	24.16	3841	8358	0.7735	4.118
MF4	0.2451	1.225	5.833	21.83	3368	12140	0.6087	3.898
MF5	0.1984	1.408	2.718	23.25	3283	23480	0.2106	3.382
MF6	0.345	1.306	4.921	23.55	5720	43740	0.243	3.551
MF7	0.3369	0.9932	5.99	28.2	3841	30940	0.4181	2.848
MF8	0.2285	1.577	5.553	34.41	6493	47470	0.2283	3.614
MF9	0.4052	1.383	7.403	25.74	4509	36160	0.2132	3.592
MF10	0.5183	1.363	7.66	26.82	3209	14850	1.021	3.501
MF11	0.0936	1.465	3.624	15.48	3211	21820	0.2024	3.488
MF12	0.2993	1.627	4.018	25.18	5193	40810	0.1552	3.481
MF13	0.2519	1.586	4.19	30.24	3558	28020	0.2193	3.461
MF14	0.38	1.528	5.433	25.78	3142	18110	0.1825	3.22
MF15	0.341	0.2856	3.052	28.99	3400	25730	0.4339	2.224

n represents the Gaussian MF width, *M* determines the Gaussian MF center

Table 4 Parameters of the membership functions for modeling the pressure drop of the titanium dioxide–water nanofluids

Membership function	Input 1 ϕ (%)		Input 2 d_p(nm)		Input 3 *Re*	
	n	*M*	*n*	*M*	*n*	*M*
MF1	0.4	1.383	6.007	28.43	6350	44850
MF2	0.2612	1.002	5.477	26.97	4126	31300
MF3	0.1906	1.646	6.592	25.45	4962	37440
MF4	2.016	0.8562	11.88	22.97	4773	5082
MF5	1.172	1.517	3.703	23.24	3769	11910
MF6	0.5482	1.289	4.78	27.04	3571	20100
MF7	0.7903	1.261	4.263	29.63	3571	15140
MF8	0.8266	0.6216	8.065	27.14	3657	25250
MF9	1.172	1.877	10.08	24.1	4157	8377
MF10	0.4059	1.756	10.1	29.93	3774	27640

n represents the Gaussian MF width, *M* determines the Gaussian MF center

Table 5 Fuzzy rule base and ANFIS output for modeling the Nusselt number of the titanium dioxide–water nanofluids

Number of Rules	Rule description
1	If (ϕ is ϕ MF1) and (d_p is d_p MF1) and (Re is Re MF1) and (Pr is Pr MF1) then $Nu_{nf} = a_{1,1}.\ \phi + a_{1,2}.\ d_p + a_{1,3}.\ Re + a_{1,4}.\ Pr + a_{1,5}$
2	If (ϕ is ϕ MF2) and (d_p is d_p MF2) and (Re is Re MF2) and (Pr is Pr MF2) then $Nu_{nf} = a_{2,1}.\ \phi + a_{2,2}.\ d_p + a_{2,3}.\ Re + a_{2,4}.\ Pr + a_{2,5}$
3	If (ϕ is ϕ MF3) and (d_p is d_p MF3) and (Re is Re MF3) and (Pr is Pr MF3) then $Nu_{nf} = a_{3,1}.\ \phi + a_{3,2}.\ d_p + a_{3,3}.\ Re + a_{3,4}.\ Pr + a_{3,5}$
4	If (ϕ is ϕ MF4) and (d_p is d_p MF4) and (Re is Re MF4) and (Pr is Pr MF4) then $Nu_{nf} = a_{4,1}.\ \phi + a_{4,2}.\ d_p + a_{4,3}.\ Re + a_{4,4}.\ Pr + a_{4,5}$
5	If (ϕ is ϕ MF5) and (d_p is d_p MF5) and (Re is Re MF5) and (Pr is Pr MF5) then $Nu_{nf} = a_{5,1}.\ \phi + a_{5,2}.\ d_p + a_{5,3}.\ Re + a_{5,4}.\ Pr + a_{5,5}$
6	If (ϕ is ϕ MF6) and (d_p is d_p MF6) and (Re is Re MF6) and (Pr is Pr MF6) then $Nu_{nf} = a_{6,1}.\ \phi + a_{6,2}.\ d_p + a_{6,3}.\ Re + a_{6,4}.\ Pr + a_{6,5}$
7	If (ϕ is ϕ MF7) and (d_p is d_p MF7) and (Re is Re MF7) and (Pr is Pr MF7) then $Nu_{nf} = a_{7,1}.\ \phi + a_{7,2}.\ d_p + a_{7,3}.\ Re + a_{7,4}.\ Pr + a_{7,5}$
8	If (ϕ is ϕ MF8) and (d_p is d_p MF8) and (Re is Re MF8) and (Pr is Pr MF8) then $Nu_{nf} = a_{8,1}.\ \phi + a_{8,2}.\ d_p + a_{8,3}.\ Re + a_{8,4}.\ Pr + a_{8,5}$
9	If (ϕ is ϕ MF9) and (d_p is d_p MF9) and (Re is Re MF9) and (Pr is Pr MF9) then $Nu_{nf} = a_{9,1}.\ \phi + a_{9,2}.\ d_p + a_{9,3}.\ Re + a_{9,4}.\ Pr + a_{9,5}$
10	If (ϕ is ϕ MF10) and (d_p is d_p MF10) and (Re is Re MF10) and (Pr is Pr MF10) then $Nu_{nf} = a_{10,1}.\ \phi + a_{10,2}.\ d_p + a_{10,3}.\ Re + a_{10,4}.\ Pr + a_{10,5}$
11	If (ϕ is ϕ MF11) and (d_p is d_p MF11) and (Re is Re MF11) and (Pr is Pr MF11) then $Nu_{nf} = a_{11,1}.\ \phi + a_{11,2}.\ d_p + a_{11,3}.\ Re + a_{11,4}.\ Pr + a_{11,5}$
12	If (ϕ is ϕ MF12) and (d_p is d_p MF12) and (Re is Re MF12) and (Pr is Pr MF12) then $Nu_{nf} = a_{12,1}.\ \phi + a_{12,2}.\ d_p + a_{12,3}.\ Re + a_{12,4}.\ Pr + a_{12,5}$
13	If (ϕ is ϕ MF13) and (d_p is d_p MF13) and (Re is Re MF13) and (Pr is Pr MF13) then $Nu_{nf} = a_{13,1}.\ \phi + a_{13,2}.\ d_p + a_{13,3}.\ Re + a_{13,4}.\ Pr + a_{13,5}$
14	If (ϕ is ϕ MF14) and (d_p is d_p MF14) and (Re is Re MF14) and (Pr is Pr MF14) then $Nu_{nf} = a.{}_{14,1}.\ \phi + a_{14,2}.\ d_p + a_{14,3}.\ Re + a_{14,4}.\ Pr + a_{14,5}$
15	If (ϕ is ϕ MF15) and (d_p is d_p MF15) and (Re is Re MF15) and (Pr is Pr MF15) then $Nu_{nf} = a_{15,1}.\ \phi + a_{15,2}.\ d_p + a_{15,3}.\ Re + a_{15,4}.\ Pr + a_{15,5}$

Table 6 Fuzzy rule base and ANFIS output for modeling the pressure drops of the titanium dioxide–water nanofluids

Number of Rules	Rule description
1	If (ϕ is ϕ MF1) and (d_p is d_p MF1) and (Re is Re MF1) then $\Delta P_{nf} = b_{1,1}.\ \phi + b_{1,2}.\ d_p + b_{1,3}.\ Re + b_{1,4}$
2	If (ϕ is ϕ MF2) and (d_p is d_p MF2) and (Re is Re MF2) then $\Delta P_{nf} = b_{2,1}.\ \phi + b_{2,2}.\ d_p + b_{2,3}.\ Re + b_{2,4}$
3	If (ϕ is ϕ MF3) and (d_p is d_p MF3) and (Re is Re MF3) then $\Delta P_{nf} = b_{3,1}.\ \phi + b_{3,2}.\ d_p + b_{3,3}.\ Re + b_{3,4}$
4	If (ϕ is ϕ MF4) and (d_p is d_p MF4) and (Re is Re MF4) then $\Delta P_{nf} = b_{4,1}.\ \phi + b_{4,2}.\ d_p + b_{4,3}.\ Re + b_{4,4}$
5	If (ϕ is ϕ MF5) and (d_p is d_p MF5) and (Re is Re MF5) then $\Delta P_{nf} = b_{5,1}.\ \phi + b_{5,2}.\ d_p + b_{5,3}.\ Re + b_{5,4}$
6	If (ϕ is ϕ MF6) and (d_p is d_p MF6) and (Re is Re MF6) then $\Delta P_{nf} = b_{6,1}.\ \phi + b_{6,2}.\ d_p + b_{6,3}.\ Re + b_{6,4}$
7	If (ϕ is ϕ MF7) and (d_p is d_p MF7) and (Re is Re MF7) then $\Delta P_{nf} = b_{7,1}.\ \phi + b_{7,2}.\ d_p + b_{7,3}.\ Re + b_{7,4}$
8	If (ϕ is ϕ MF8) and (d_p is d_p MF8) and (Re is Re MF8) then $\Delta P_{nf} = b_{8,1}.\ \phi + b_{8,2}.\ d_p + b_{8,3}.\ Re + b_{8,4}$
9	If (ϕ is ϕ MF9) and (d_p is d_p MF9) and (Re is Re MF9) then $\Delta P_{nf} = b_{9,1}.\ \phi + b_{9,2}.\ d_p + b_{9,3}.\ Re + b_{9,4}$
10	If (ϕ is ϕ MF10) and (d_p is d_p MF10) and (Re is Re MF10) then $\Delta P_{nf} = b_{10,1}.\ \phi + b_{10,2}.\ d_p + b_{10,3}.\ Re + b_{10,4}$

Table 7 Values of the design variables (input variables) and objective functions at the start and end section points

Points	ϕ (%)	d_p (nm)	*Re*	*Pr*	*Nu*	Δ*P* (kPa)
A	1.5	34	22143	3.5	207.856	1.187
B	1.5	35	233333	3.5	265.599	4.629
C	1.17	20	20159	3.5	274.492	5.197
D	1.5	24	22937	3.5	519.964	9.027

List of Figure captions

Figure 1 Comparison of the experimental data of Sajadi and Kazemi [19] with the proposed FCM-ANFIS model for the Nusselt number and existing correlations (titanium dioxide–water nanofluid with an average particle size of 30 nm at a volume concentration of 0.1%)

Figure 2 Comparison of the experimental data of Duangthongsuk and Wongwises [17] with the proposed FCM-ANFIS model for the Nusselt number and existing correlations (titanium dioxide–water nanofluid with an average particle size of 21 nm at a volume concentration of 0.6%)

Figure 3 Comparison of the experimental data of Abbasian Arani and Amani [21] with the proposed FCM-ANFIS model for the Nusselt number and existing correlations (titanium dioxide–water nanofluid with an average particle size of 50 nm at a volume concentration of 1.5%)

Figure 4 Comparison of the experimental data of Abbasian Arani and Amani [21] with the proposed FCM-ANFIS model for the Nusselt number and existing correlations (titanium dioxide–water nanofluid with an average particle size of 10 nm at a volume concentration of 2%)

Figure 5 Comparison of the experimental data with the proposed FCM-ANFIS model for the pressure drop (a- titanium dioxide–water nanofluid with an average particle size of 30 nm at a volume concentration of 0.15% [19] b- titanium dioxide–water nanofluid with an average particle size of 21 nm at a volume concentration of 0.2% [17] c- titanium dioxide–water nanofluid with an average particle size of 50 nm at a volume concentration of 1% [21] d- titanium dioxide–water nanofluid, with an average particle size of 10 nm at a volume concentration of 1.5% [21])

Figure 6 Multi-objective Pareto front of the Nusselt number and pressure drop

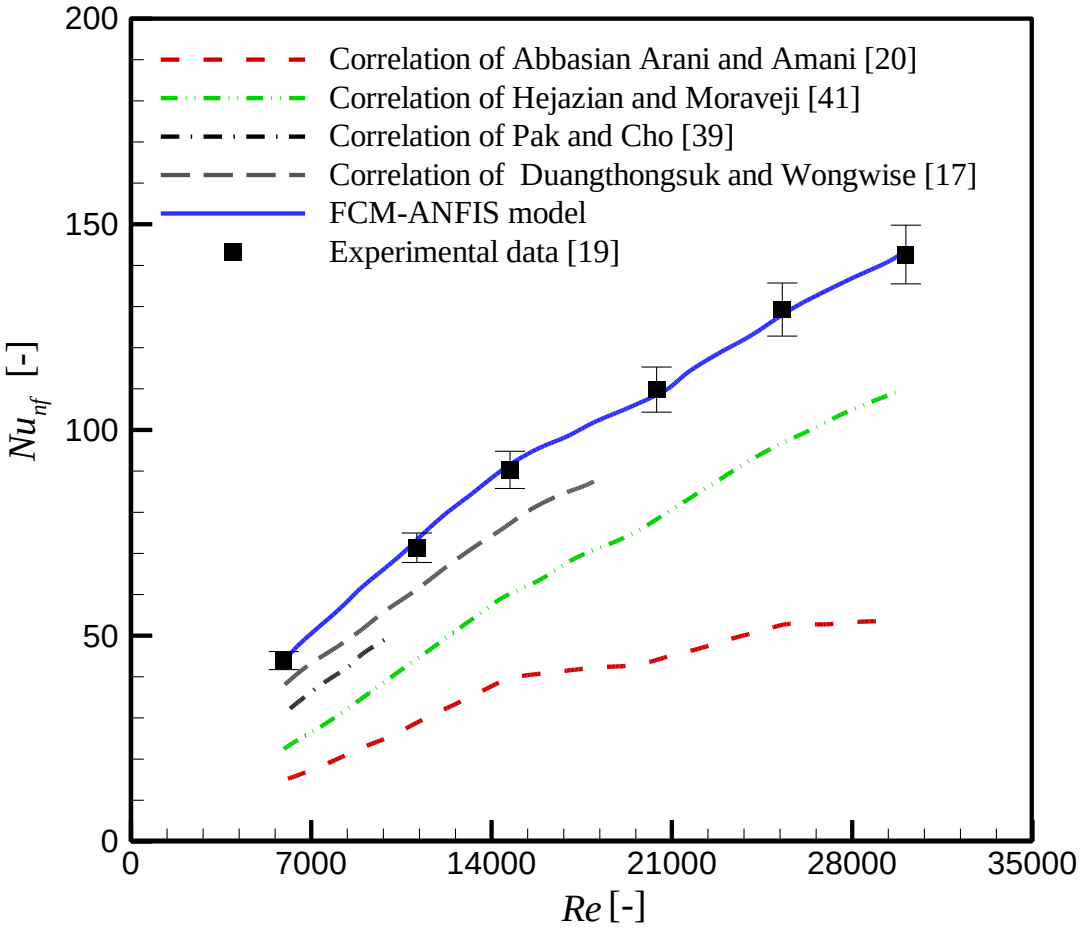

Figure 1 Comparison of the experimental data of Sajadi and Kazemi [19] with the proposed FCM-ANFIS model for the Nusselt number and existing correlations (titanium dioxide–water nanofluid with an average particle size of 30 nm at a volume concentration of 0.1%)

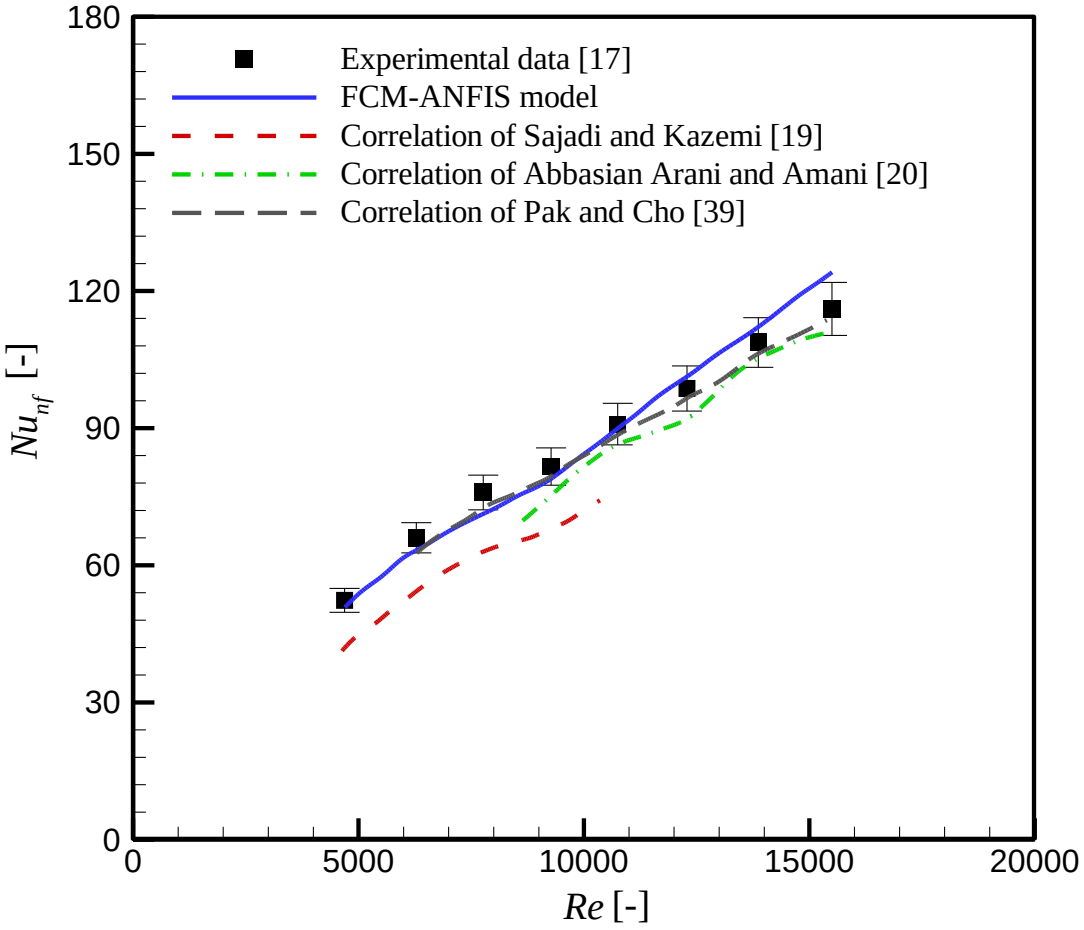

Figure 2 Comparison of the experimental data of Duangthongsuk and Wongwises [17] with the proposed FCM-ANFIS model for the Nusselt number and existing correlations (titanium dioxide–water nanofluid with an average particle size of 21 nm at a volume concentration of 0.6%)

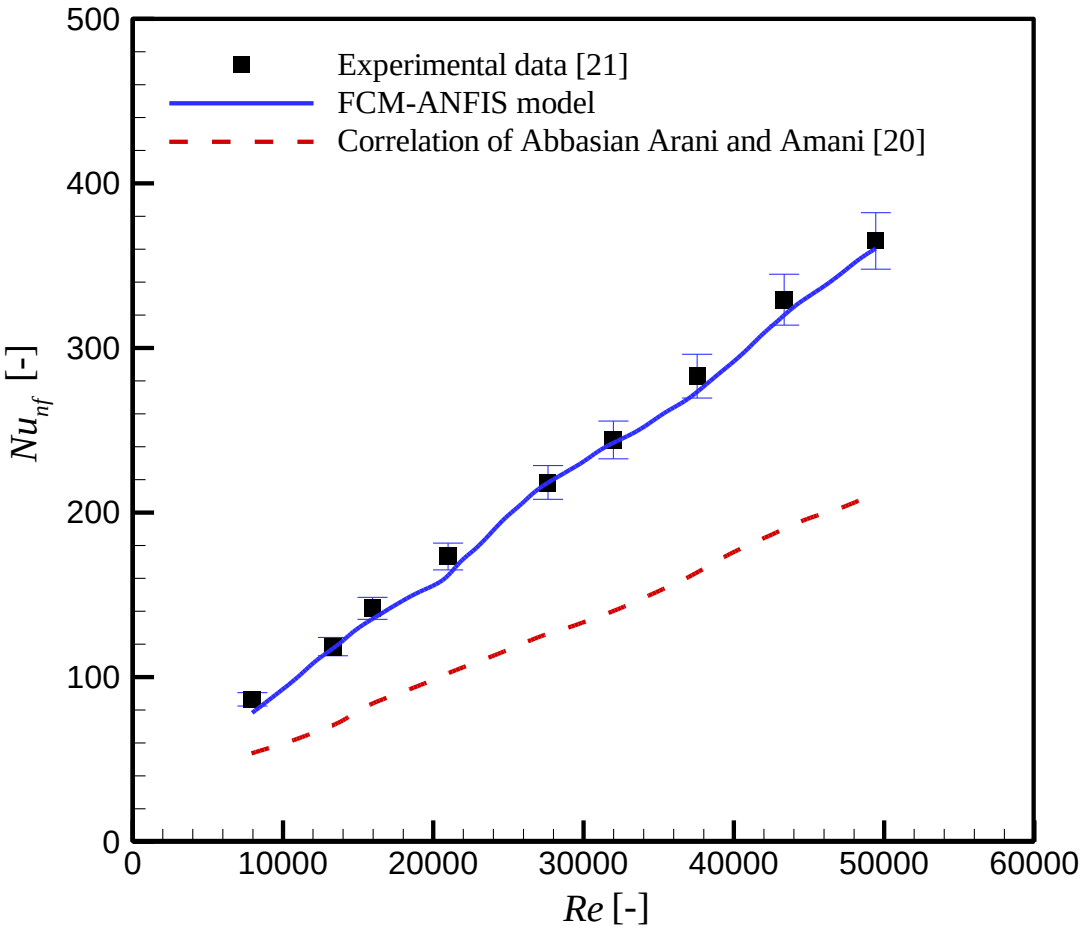

Figure 3 Comparison of the experimental data of Abbasian Arani and Amani [21] with the proposed FCM-ANFIS model for the Nusselt number and existing correlations (titanium dioxide–water nanofluid with an average particle size of 50 nm at a volume concentration of 1.5%)

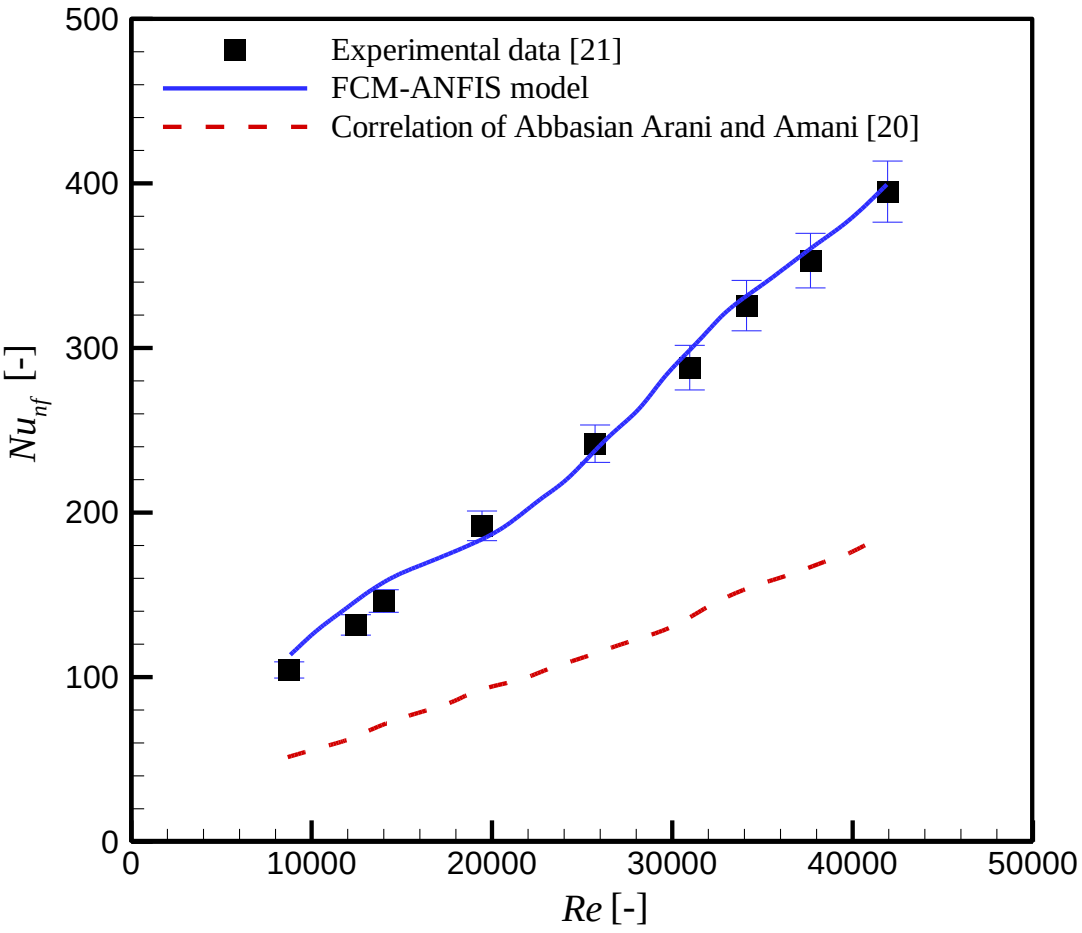

Figure 4 Comparison of the experimental data of Abbasian Arani and Amani [21] with the proposed FCM-ANFIS model for the Nusselt number and existing correlations (titanium dioxide–water nanofluid with an average particle size of 10 nm at a volume concentration of 2%)

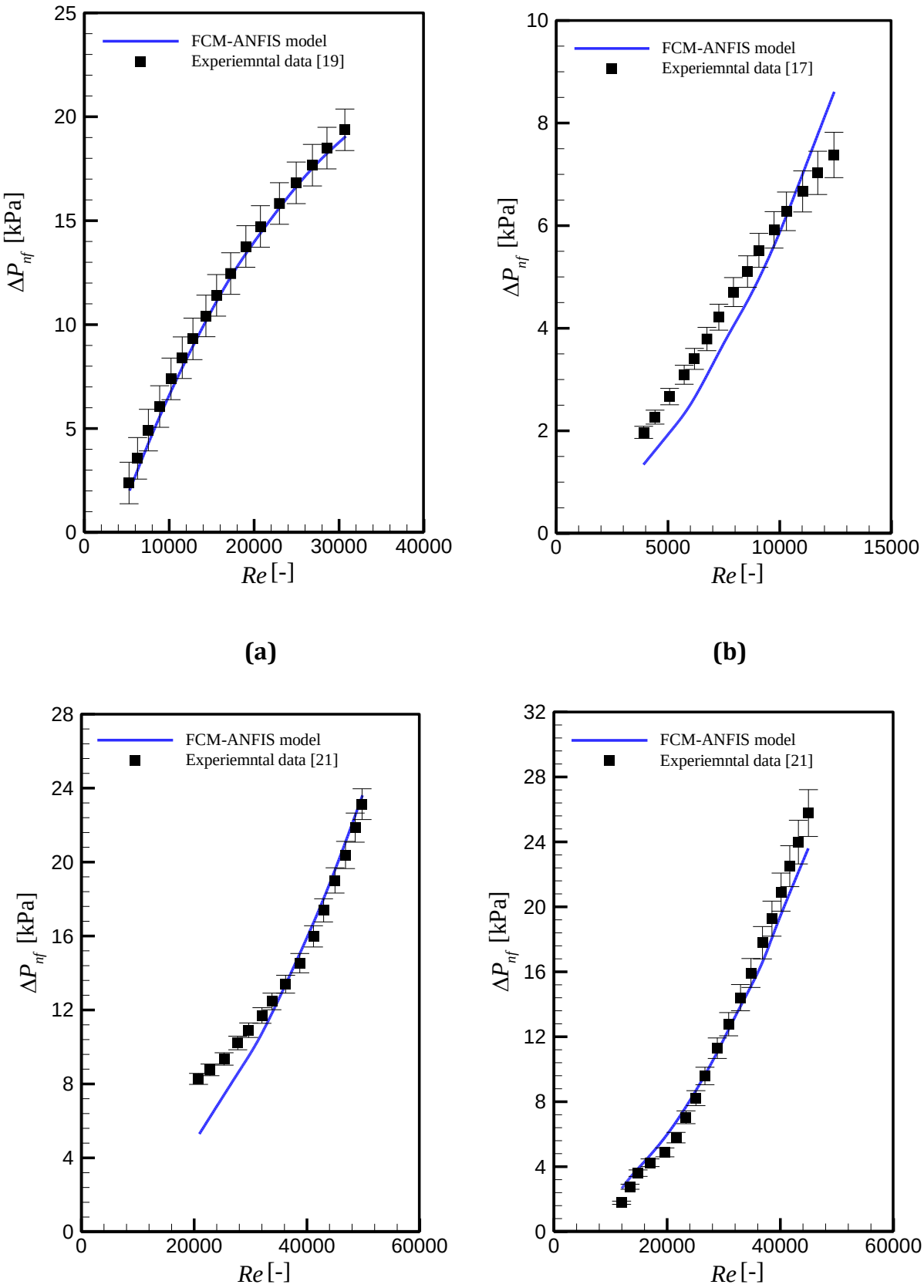
FCM-ANFIS model
Experiemntal data [19]
ΔP_{nf} [kPa]
Re [-]
(a)
FCM-ANFIS model
Experiemntal data [17]
ΔP_{nf} [kPa]
Re [-]
(b)
FCM-ANFIS model
Experiemntal data [21]
ΔP_{nf} [kPa]
Re [-]
(c)
FCM-ANFIS model
Experiemntal data [21]
ΔP_{nf} [kPa]
Re [-]
(d)

Figure 5

Figure 5 Comparison of the experimental data with the proposed FCM-ANFIS model for the pressure drop (a- titanium dioxide–water nanofluid with an average particle size of 30 nm at a volume concentration of 0.15% [19] b- titanium dioxide–water nanofluid with an average particle size of 21 nm at a volume concentration of 0.2% [17] c- titanium dioxide–water nanofluid with an average particle size of 50 nm at a volume concentration of 1% [21] d- titanium dioxide–water nanofluid, with an average particle size of 10 nm at a volume concentration of 1.5% [21])

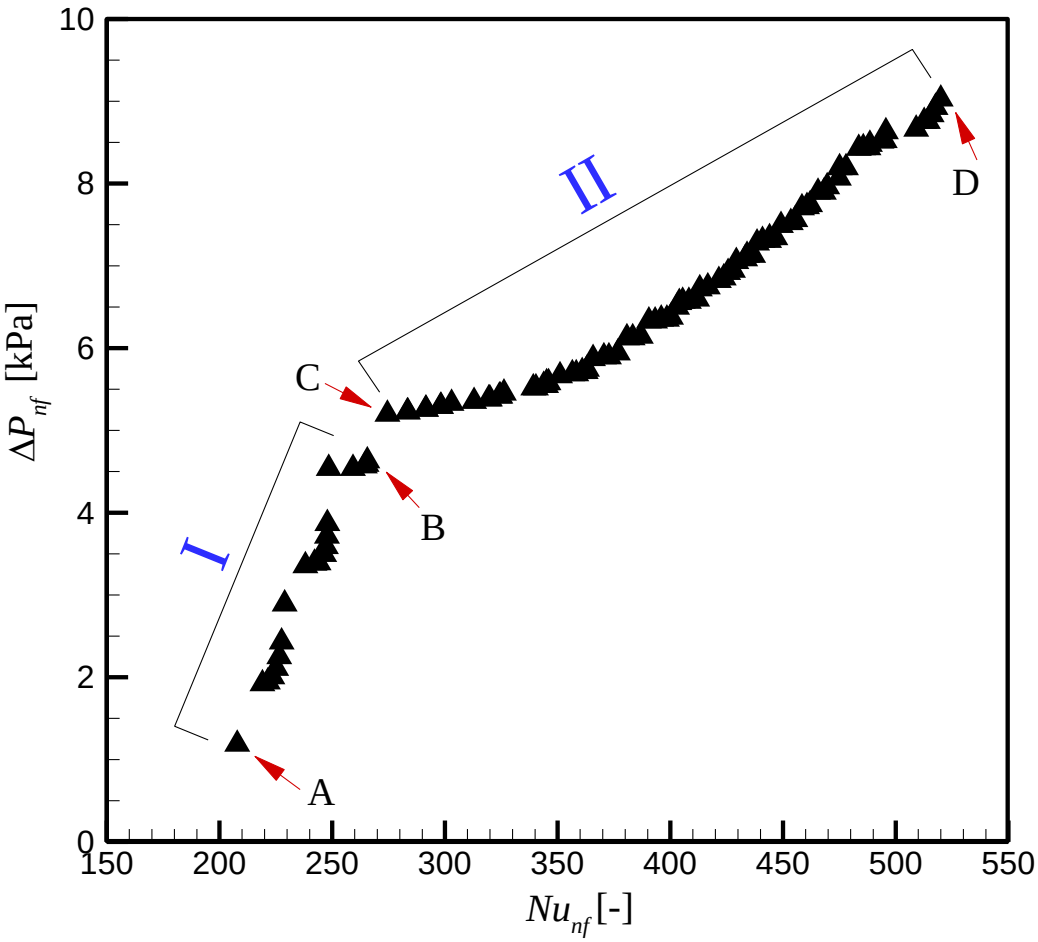

Figure 6 Multi-objective Pareto front of the Nusselt number and pressure drop

Mehdi Mehrabi obtained his B.Eng. in Mechanical Engineering (Heat and Fluid Flow) in 2006 and his M.Eng. in Mechanical Engineering (Energy Conversion) in 2011, both from Urmia University, Urmia, Iran and Ph.D. in Mechanical Engineering from the University of Pretoria, South Africa in 2015. He joined the Department of Mechanical and Aeronautical Engineering at the University of Pretoria, South Africa as a Senior Lecturer in 2017. He is a member of the Clean Energy Research Group and his research interests include, convection heat transfer, multi-objective optimization techniques, application of artificial intelligence techniques for modeling heat transfer processes, and thermophysical properties of nanofluids.

Seyyed Mohammad Ali Noori Rahim Abadi is an expert in multiphase computational fluid dynamics. He received his Ph.D. in Mechanical Engineering from the University of Guilan in 2015. After receiving his Ph.D., he joined the Clean Energy Research Group of the University of Pretoria as a postdoctoral fellow. He has extensive academic and industrial experience in the field of thermal-fluid sciences. His research interests encompass multiphase flows, heat and mass transfer, and thermodynamics.

J. P. Meyer is a Professor and the Head of the Department of Mechanical and Aeronautical Engineering and Chair of the School of Engineering at the University of Pretoria. His research field is convective heat transfer in which he has published more than 600 scholarly articles, conference papers and book chapters. He has successfully supervised more than 100 postgraduate students for research masters and Ph.D.'s. He has received various international awards for his research. According to the Essential Science Indicators of the ISI Web of Knowledge he is ranked

amongst the top 1% of the world in engineering in all the three evaluation fields of citations, number of papers and citations per paper. He is/was the editor, lead editor, and associate editor of various prominent international heat transfer journals.

ORCID

M. Mehrabi 0000-0003-3027-2560

S. M. A. Noori Rahim Abadi 0000-0002-6102-9021

J.P. Meyer 0000-0002-3675-5494